# Adipic acid assisted sol–gel synthesis of $Li_2MnSiO_4$ nanoparticles with improved lithium storage properties

V. Aravindan,†[a] K. Karthikeyan,[a] S. Ravi,[b] S. Amaresh,[a] W. S. Kim[c] and Y. S. Lee*[a]

*Received 28th May 2010, Accepted 15th July 2010*
**DOI: 10.1039/c0jm01635g**



**An adipic acid assisted sol–gel route was employed to prepare phase pure $Li_2MnSiO_4$ under the optimized conditions. Powder X-ray diffraction measurements confirm the formation of orthorhombic $Li_2MnSiO_4$ with *Pmn2₁* space group. The oxidation state of Mn(II) was confirmed by electron paramagnetic resonance (EPR) studies. FTIR study was conducted to ensure the formation of a tetrahedral $SiO_4$ group. Morphological features confirmed the appearance of evenly dispersed $Li_2MnSiO_4$ spherical nanoparticles with size of ~30 nm. The Li/$Li_2MnSiO_4$ cell was constructed to study the electrochemical performance of $Li_2MnSiO_4$ nanoparticles and the cell delivers a stable discharge capacity profile (~125 mAh $g^{-1}$) for observed 50 cycles.**

## 1 Introduction

Lithium orthosilicates, $Li_2MSiO_4$ (M = Fe, Mn, Co and Ni), have recently attracted the attention of researchers due to their appealing properties like high theoretical capacity (>300 mAh $g^{-1}$), plausible extraction of more than one $Li^+$ ion per formula unit and high thermal stability through strong Si–O bonding.[1] Among the silicate groups, $Li_2FeSiO_4$ and $Li_2MnSiO_4$ are more attractive than other counterparts because they are more cost effective and environmentally benign.[1–10] However, $Li_2MnSiO_4$ provides a higher cell voltage due to the possible oxidation of the $Mn^{3+}/Mn^{4+}$ couple rather than $Fe^{2+}/Fe^{3+}$.[7–10] All the orthosilicate candidates also suffered due to the inherent conducting properties, such as that of olivine phosphates. In olivine phosphates, particularly, $LiFePO_4$, the conducting problem was circumvented by surface modification especially carbon coating, which dramatically improves the cycleability and rate performance of the cell.[11] A similar approach is expected here to improve the electrochemical properties of the cell.

Only very few reports could be found on the synthesis and characterization of $Li_2MnSiO_4$ either by solid state or sol–gel route.[2–10,12–14] These two routes are suitable for mass production of the materials in industries. Furthermore, the sol–gel route is a convenient procedure to synthesize the desired size of particles having good stoichiometry and morphology than solid-state approach. Previously, Jamnik an co-workers[3] reported the synthesis of $Li_2MnSiO_4$ by a modified Pechni sol–gel route, in this process, $SiO_2$ is dispersed in water and Mn and Li source materials were added to form a gel and finally heat treated to yield the resultant product. But, in such processes, a real solution phase reaction does not take place, which is also similar to that of solid state reaction method. Li *et al.*[12] also reported the solution phase sol–gel route by using tetraethoxysilane as source material for silicon. However, that report presented the poor cycling performance of the cell, which may be due to either the starting material or poor optimization. Belharouak *et al.*[10] reported the sol–gel synthesized $Li_2MnSiO_4$, but failed to control the morphologies, which leads to aggregation of the resultant material. Furthermore, ball milling was employed for the carbon coating after the aggregation takes place, which in turn provides the heterogeneous coating. Recently, Deng *et al.*[14] also reported the citric acid assisted sol–gel synthesis of $Li_2MnSiO_4$ nanoparticles and their severe capacity fade during cycling, which is due to the poor optimization of the synthesis conditions. In this communication, an attempt has been made to control the morphology though optimizing the temperature and carbon coating (*in situ*) in real solution phase reaction by sol–gel route to effectively improve the performance of the cell.

## 2 Experimental section

$Li_2MnSiO_4$ nanoparticles were synthesized from the starting materials of $LiCH_3COO$ (Sigma-Aldrich, USA), $Si(CH_3COO)_4$ (Sigma-Aldrich, USA), $Mn(CH_3COO)_2$ (Sigma-Aldrich, USA), and $C_6H_{10}O_4$ (Sigma-Aldrich, USA) using a conventional sol–gel method. A stoichiometric amount of each material was dissolved in ethanol and mixed well with an aqueous solution of adipic acid (as a gelating agent, 0.2 mol against total metal ions present in $Li_2MnSiO_4$). The mixture was evaporated at 90 °C to form a transparent sol. Then, the sol was transferred to vacuum oven and dried at 90–100 °C to obtain the gel precursors. The resulting precursor was finely ground and calcined at 700 °C for 5 h in Ar atmosphere to yield the final product. The detailed experimental procedures are available in our previous work.[7]

## 3. Results and discussion

Thermogravimetric analysis (TGA) was used to ascertain the temperature conditions for the synthesis of $Li_2MnSiO_4$ nanoparticles. Fig. 1a shows the TG trace performed on the $Li_2MnSiO_4$ source materials with adipic acid, which is clearly separated by two main stages of thermal events. The first stage, comprising endothermic events, starts at ~50 °C and it showed a gradual weight loss up to ~300 °C. These initial weight losses are ascribed to the

[a]*Faculty of Applied Chemical Engineering, Chonnam National University, Gwang-ju, 500-757, South Korea. E-mail: leeys@chonnam.ac.kr*
[b]*Department of Physics, Mepco Schlenk Engineering College, Sivakasi, 626005, India*
[c]*Dajung EM Co. Ltd., Incheon 405-820, Korea*
† *Present Address*: Energy Research Institute, Nanyang Technological University, Singapore 639798, Singapore. E-mail: aravind_van@yahoo.com

 

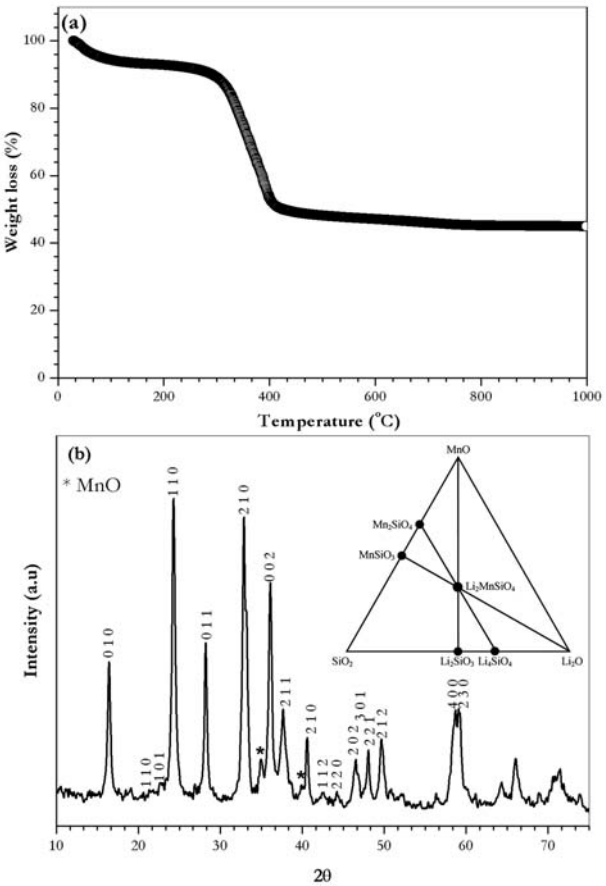


**Fig. 1** (a) Thermogravimetric traces of starting materials for synthesis of $Li_2MnSiO_4$ in an Ar atmosphere and the molar ratio of adipic acid to total metal ions is 0.2, and (b) powder X-ray diffraction pattern of synthesized $Li_2MnSiO_4$ nanoparticles at 700 °C in Ar atmosphere. The inset shows the ternary phase diagram formation $Li_2MnSiO_4$ and possible impurities.

dehydration and decomposition of acetate groups from the starting materials, as well as to the melting of adipic acid. The second thermal event exhibited a sharp endotherm (~43% weight loss) around ~300 to 430 °C, which can be recognized by decomposition of remaining reactants from the source materials as well as the carbonization of adipic acid. Thereafter, no noticeable thermal events were observed, which confirm the formation of $Li_2MnSiO_4$ nanoparticles beyond 430 °C. A serious of compounds were prepared from 600 °C to 900 °C in order to optimize the temperature condition for the synthesis of phase pure $Li_2MnSiO_4$. The optimization was carried out, based on phase purity and its battery performance. From the optimization, 700 °C is found to be the optimal condition to accomplish the high purity $Li_2MnSiO_4$ nanoparticles.

Fig. 1b shows the powder X-ray diffraction pattern of synthesized $Li_2MnSiO_4$ with phase diagram. The XRD reflections showed a well defined sharp intense peaks, which indicates the crystalline nature of the synthesized $Li_2MnSiO_4$. And there are no reflections of the starting materials used. The crystalline peaks are indexed according to the orthorhombic structure ($Li_2MnSiO_4$ with a $Li_3PO_4$ structure) with $Pmn2_1$ space group.[10] The $Li_2MnSiO_4$ can be isostructural to certain forms of $Li_3PO_4$ : $Mn^{2+}$ ions are present within a [$SiO_4$] anionic silicate network that replaces [$PO_4$] anionic phosphate network, and two Li ions are available in 3D dimensional channels. Furthermore, we believe that the strong Si–O bonds may translate into very stable electrochemical and thermal properties, *i.e.* safety issues. However, the impurity phase, like MnO, is also unavoidably present in the prepared phase. Similar kinds of impurity phases were also noticed by other researchers during synthesis of $Li_2MnSiO_4$ powders by various approaches,[1–10,12–14] de Dompablo *et al.*[9] has succeeded to prepare a $Li_2MnSiO_4$ material in the absence of MnO under various pressure conditions. Nevertheless, the formation of $Mn_2SiO_3$ could be inevitable under such abnormal pressure conditions. In addition to that, the presence of a $Mn_2SiO_3$ phase is much more prevalent than those of MnO in the conventional synthesis, either by solid state or sol–gel routes.[1–10,13] The obtained XRD pattern of $Li_2MnSiO_4$ nanoparticles reveals the purest pattern reported anywhere. In order to confirm the purity of the pattern observed from this synthesis, spectroscopic tools are used to verify the phase pure nature of $Li_2MnSiO_4$. The phase diagram clearly shows the possible formation of impurity phases during the synthesis process. From this study and based on the previous reports confirm the preparation of 100% phase pure $Li_2MnSiO_4$ is complicated one.

In order to realize the presence of Mn(II), the electron paramagnetic resonance (EPR) was utilized and is given in Fig. 2a. EPR is

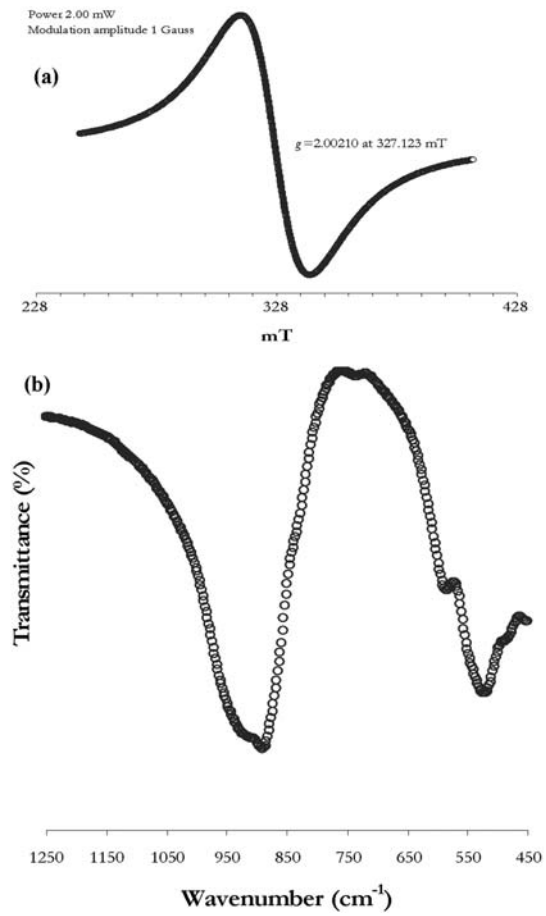


**Fig. 2** (a) Electron paramagnetic resonance (EPR) curves of $Li_2MnSiO_4$ recorded at room temperature with the power of 2 mW and modulation of amplitude of 1 gauss, and (b) Fourier transform infra-red signatures of $Li_2MnSiO_4$ nanoparticles.

an excellent tool to localize the state of any paramagnetic element present in the host manganese, which occurs in nature with various oxidation states (+1 to +6) depending on charge compensation with the ligands. Since it is a divalent ion, it quickly tries to enter the compound in 2+ oxidation states but sometimes this may change due to the surrounding environment and symmetry. Since it is purely based on spin, the results give accurate and non speculative information regarding the nature and details of an element which possess net spin. As we know manganese readily exhibits a 2+ oxidation state, it gives 30 hyperfine lines in EPR spectrum (spin S = 5/2 and I = 5/2) with 6 main hyperfine lines (if it has perfect cubic symmetry) and each main hyperfine line comprises 5 lines which may sometimes become difficult to resolve. Fig. 2a shows single broad line centered at $g = 2.00$ indicates the existence of $Mn^{2+}$ state. It appears that is sufficient lattice disorder to introduce well defined lower symmetry crystal field which broaden and eliminate other observability expect $M_S = +1/2 \leftrightarrow M_S = -1/2$ transition. This was proven in many spinel based systems since the oxygen bond surrounding manganese is difficult to study.[15,16] In our present study, manganese exhibits perfect cubic symmetry with single broad peak centered at g ≅ 2.0 which is good fit for $Mn^{2+}$ in cubic symmetry. Thus it is reasonable to assume that manganese is present in our system in 2+ oxidation state. The formation of tetrahedral $SiO_4$ group was confirmed by FTIR studies and presented in Fig. 2b. The vibrational band ~ 900 $cm^{-1}$ is attributed to the stretching vibration of O–Si–O bonds.[17] The adsorption band for stretching vibration of Si–O–Si bonds is higher than that of O–Si–O bonds and the adsorption band around 735 $cm^{-1}$ is attributed to the bending vibration of Si–O–Si bonds in tetrahedral $SiO_4$ group.[17,18] These spectroscopic investigations confirm the formation of orthorhombic $Li_2MnSiO_4$ and analogous to XRD results.

Morphological features of the synthesized $Li_2MnSiO_4$ nanoparticles are given in Fig. 3a. It obviously that the particles exhibit a spherical shape morphology without any aggregation. Highly mono dispersed particulate morphology was achieved by selecting the appropriate gelating agent with optimal concentration during the synthesis process. For the preparation of spherical $Li_2MnSiO_4$ nanoparticles, carbon rich adipic acid was chosen with 0.2 mol. against the total metal ions present in the composition (Li, Mn and Si). The uniform sized spherical $Li_2MnSiO_4$ nanoparticles exhibits the sizes around 25–30 nm. Energy dispersive X-ray spectroscopy (EDX) was also conducted for the $Li_2MnSiO_4$ nanoparticles. This spectrum was recorded against the X-ray emission of element present in the specimen as a function of electron volt (eV) and presented in Fig. 3b.

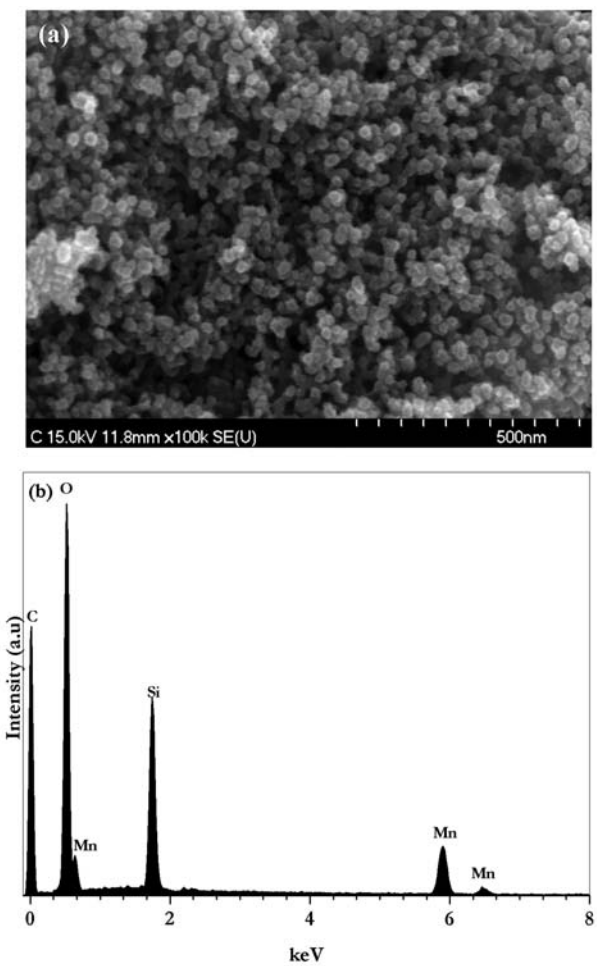


**Fig. 3** (a) Scanning electron microscopic pictures of $Li_2MnSiO_4$ spherical nanoparticles synthesized at 700 °C in Ar atmosphere and (b) energy dispersive X-ray spectroscopy patterns of $Li_2MnSiO_4$ nanoparticle.

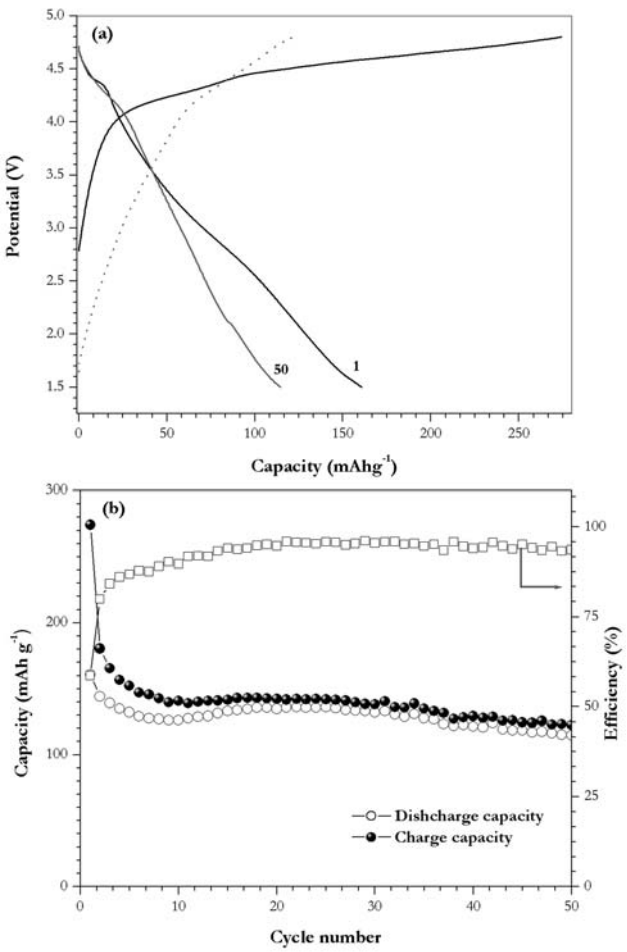


**Fig. 4** (a) Typical charge-discharge capacity curves of Li/$Li_2MnSiO_4$ cell at room temperature conditions by C/20 rate, and (b) cycling profiles of Li/$Li_2MnSiO_4$ cells with efficiency.

 

The EDX spectrum indicates the presence of carbon along with the prepared $Li_2MnSiO_4$. The presence of carbon might be from the carbonization of gelating agent *i.e.* adipic acid at high temperature sintering, which may form on the surface of the particles. In other words, the *in situ* carbon coating has been achieved during the synthesis process. For this reason, the choice of gelating agent plays a vital role to determine the electrochemical properties of the material prepared. Adipic acid is an excellent source material for gelating agent as well as carbon source and this was convincingly proven for the synthesis of $LiFePO_4$ either by solid state[19] or by sol gel[20] by our group. Generally, a carbon coating may be employed after the synthesis and mixed with appropriate amount of carbon, ball milled and finally heat treated at certain temperature. However, in such process, the coating may not be in uniform and the particle morphology is also affected during the milling procedure.

Fig. 4 illustrates the electrochemical performance of the Li/$Li_2MnSiO_4$ cell at room temperature. The Li/$Li_2MnSiO_4$ cell was cycled between 1.5–4.8 V at C/20 rate. The cell delivers the initial discharge capacity of 161 mAh $g^{-1}$ against charge capacity of 274 mAh $g^{-1}$. $Li_2MnSiO_4$ offered a high theoretical capacity of 333 mAh $g^{-1}$ and possible extraction of more than one $Li^+$ ion per unit formula is plausible. In the case of lithium battery cathodes theoretical capacity is very rarely achieved, for example $LiFePO_4$.[12] The Li/$Li_2MnSiO_4$ cell, during first charge only, the extraction beyond one $Li^+$ ion per formula unit is realized (1.65 $Li^+$ ions), whereas 0.97 $Li^+$ ions per formula unit only reinserted into the host matrix. Some lithium ions may involve to the formation of stable solid electrolyte interphase (SEI), which is also one of the reasons for the poor efficiency in the first cycle. A similar kind of poor cycling efficiency in Li/$Li_2MnSiO_4$ cell is also observed by other authors.[6,13] In the initial cycles, a gradual decrease in discharge capacity profile is observed for few cycles until the formation of stable SEI. After the formation of stable SEI, columbic efficiency of the cell is over 95%. Almost a stable performance is observed for the tested 50 cycles and this is one of the best results achieved for $Li_2MnSiO_4$ materials. At the end of 50th cycle the Li/$Li_2MnSiO_4$ cell experienced the discharge capacity of 115 mAh $g^{-1}$ (charge capacity 121 mAh $g^{-1}$) with the columbic efficiency of 95%. So far, no work has been reported for such a stable behavior beyond 10 cycles.[1–10] This improved performance may be attributed to the carbonization getaling agent *i.e.* adipic acid, which may form as a thin layer of carbon on the surface of the particles. The EDX pattern confirms the presence of carbon during the synthesis process. At the same time, orthosilicates also experience the poor conductivity problem, which is similar to that of $LiFePO_4$.[6] The same kind of procedure was adopted here to circumvent the inherent conducting properties of $Li_2MnSiO_4$ as that of $LiFePO_4$. Further, carbon coating provides the improvement in electronic conductivity of the $Li_2MnSiO_4$ materials, which reflected in the electrochemical studies. The size effect of $Li_2MnSiO_4$ materials cannot be excluded for the improvement in the discharge capacity profile.[11] The presence of carbon also prevents the unwanted side reaction with electrolyte which leads to increase in the life of the cell. Moreover, the source of carbon is also very important. We varied the concentration of gelating agent from 0 mol (against total metal ion present in $Li_2MnSiO_4$) to 2 mol (0, 0.1, 0.2, 0.5, 1.0 and 2.0), among them, 0.2 mol adipic acid containing $Li_2MnSiO_4$ exhibited excellent performance (not shown). Increasing the concentration of gelating agent leads to the dilution of active particle distance, which in turn resulted in a poor capacity profile. Similarly, at low concentration, the carbon content is not sufficient for the coating, which also provides the poor profile. Hence, from this study we optimized the gelating agent 0.2 mol. to achieve mono dispersed $Li_2MnSiO_4$ nanoparticles having excellent battery performance without any additional treatments like *ex situ* carbon coating, ball milling and sintering *etc.*

## 4 Conclusions

$Li_2MnSiO_4$ nanoparticles were successfully synthesized by a sol–gel route in the presence of adipic acid. From the thermogravimetric studies, 700 °C could be the optimal temperature to attain the high performance nanoparticles. EPR and FTIR spectroscopic tools were used to prove the phase formation. The morphological study reveals $Li_2MnSiO_4$ nanoparticles exhibiting spherical shape with size around 25–30 nm. The Li/$Li_2MnSiO_4$ cell exhibited initial discharge capacity ~161 mAh $g^{-1}$ and delivered a stable discharge capacity profile of up to 50 cycles.

## Acknowledgements

This research work was financially supported by the Ministry of Knowledge Economy (MKE), Korea Institute for Advancement of Technology (KIAT) and Honam Leading Industry Office through the Leading Industry Development for Economic Region.

## References

1 M. E. A. de Dompablo, M. Armand, J. M. Tarascon and U. Amador, *Electrochem. Commun.*, 2006, **8**, 1292–1298.
2 A. Nytén, A. Abouimrane, M. Armand, T. Gustafsson and J. O. Thomas, *Electrochem. Commun.*, 2005, **7**, 156–160.
3 R. Dominko, M. Bele, M. Gaberšček, A. Meden, M. Remškar and J. Jamnik, *Electrochem. Commun.*, 2006, **8**, 217–222.
4 A. Kokalj, R. Dominko, G. Mali, A. Meden, M. Gaberscek and J. Jamnik, *Chem. Mater.*, 2007, **19**, 3633–3640.
5 R. Dominko, *J. Power Sources*, 2008, **184**, 462–468.
6 W. Liu, Y. Xu and R. Yang, *J. Alloys Compd.*, 2009, **480**, L1–L4.
7 K. Karthikeyan, V. Aravindan, S. B. Lee, I. C. Jang, H. H. Lim, G. J. Park, M. Yoshio and Y. S. Lee, *J. Power Sources*, 2010, **195**, 3761–3764.
8 R. Dominko, I. Arcon, A. Kodre, D. Hanzel and M. Gaberscek, *J. Power Sources*, 2009, **189**, 51–58.
9 M. E. A. de Dompablo, R. Dominko, J. M. G. Amores, L. Dupont, G. Mali, H. Ehrenberg, J. Jamnik and E. Moran, *Chem. Mater.*, 2008, **20**, 5574–5584.
10 I. Belharouak, A. Abouimrane and K. Amine, *J. Phys. Chem. C*, 2009, **113**, 20733–20737.
11 Z. Li, D. Zhang and F. Yang, *J. Mater. Sci.*, 2009, **44**, 2435–2443.
12 Y. X. Li, Z. L. Gong and Y. Yang, *J. Power Sources*, 2007, **174**, 528–532.
13 R. Dominko, M. Bele, A. Kokalj, M. Gaberscek and J. Jamnik, *J. Power Sources*, 2007, **174**, 457–461.
14 C. Deng, S. Zhang, B. L. Fu, S. Y. Yang and L. Ma, *Mater. Chem. Phys.*, 2010, **120**, 14–17.
15 L. Pawlak, K. Falkowski and S. Pokrzywnicki, *J. Solid State Chem.*, 1981, **37**, 228–231.
16 A. Abraham, B. Bleaney, *Electron Paramagnetic Resonance of Transition Ions*, Oxford University Press, 1970, pp. 447.
17 B. D. Mihailova, M. S. Marinov and L. L. Konstantinov, *J. Non-Cryst. Solids*, 1994, **176**, 127–132.
18 P. Comodi, Y. Liu, F. Stoppa and A. R. Woolley, *Mineral. Mag.*, 1999, **63**, 661–672.
19 H. H. Lim, I. C. Jang, S. B. Lee, K. Karthikeyan, V. Aravindan and Y. S. Lee, *J. Alloys Compd.*, 2010, **495**, 181–184.
20 S. B. Lee, I. C. Jang, H. H. Lim, V. Aravindan, H. S. Kim and Y. S. Lee, *J. Alloys Compd.*, 2010, **491**, 668–672.